Proc. Natl. Acad. Sci. USA
Vol. 86, pp. 7223–7227, September 1989
Neurobiology

Expression of an intrinsic growth strategy by mammalian retinal neurons

(retinal ganglion cell/cell culture/Hausdorff dimension)

P. READ MONTAGUE*† AND MICHAEL J. FRIEDLANDER*†‡

*Neurobiology Research Center and †Department of Physiology and Biophysics, University of Alabama at Birmingham, Birmingham, AL 35294

Communicated by Torsten N. Wiesel, May 30, 1989 (received for review April 25, 1989)

ABSTRACT **Postnatal cat retinal ganglion cells (RGCs) were retrogradely labeled with fluorescent microspheres, dissociated from the retina using a peeling procedure, and monitored in cell culture with a time-lapse video microscopy system. The spatial patterns formed by the growing neurites were analyzed using conventional and fractal measures (Hausdorff dimension, *H*) of their extent and complexity. The results presented were obtained from the arborizations formed by the neurites of 48 labeled and isolated ganglion cells growing separate from each other and separate from a feeder layer of astrocytes. Cells were obtained from animals when the RGCs were postmitotic and after dendritic differentiation *in vivo* at age 0–1 week (4/48), 2–5 weeks (35/48), or 6–8 weeks (9/48). By 48 hr after plating, the number of surviving labeled RGCs was reduced to 22–28% of its initial value. After removal of all processes and isolation *in vitro*, these RGCs expressed neurite patterns strikingly similar to those seen in the intact retina, although the RGCs had been deprived of potential cues from the intact retina and target tissue. Self crossings of the growing neurites were rare (<0.5%, 20 cells, n = 2500 neurites). Calculation of the Hausdorff dimension, a metric for the space-filling capacity of the neurite patterns, revealed that after 3-day culture 77% (n = 56) of the RGCs achieved relatively uniform coverage of territory ($1.6 < H < 1.9$). This coverage was independent of the number of interbranchpoint segments and/or the total neurite length of a particular neurite pattern. A sample of dendritic arbors from RGCs in intact retina yielded similar values for the Hausdorff dimension (H = 1.73, SD = 0.12, n = 18, range 1.54–1.94). These results reveal that a mammalian central nervous system neuron, for at least 8 postnatal weeks, has the intrinsic capacity for reexpression of *in vivo* structure characteristic of that cell type in the absence of interaction with neighboring neurons, afferent input, and target tissue. These neurons exhibit stereotyped growth resulting in uniform coverage of a restricted territory by the strategic selection of the length, location, and orientation of interbranchpoint segments.**

Neuronal morphology, as an emergent cellular trait, depends on a host of epigenetic infuences as well as a variety of processes that are intrinsic to the neuron (1, 2). The intrinsic control of neuronal form has always been a fundamental problem of biological development, and recently, the intrinsic capacity for neurons to develop the complex dendritic patterns characteristic of certain central nervous system sites has been demonstrated in cell culture (3-9). This development occurs in spite of isolation from epigenetic influences from other neurons and is most robust in cells derived from prenatal animals after commitment to the neuronal lineage and yet before extensive dendritic differentiation (9, 10). However, the degree to which this intrinsic capacity is retained after the expression of mature dendritic structure and function is unknown. Moreover, the existence of local and/or global strategies for the elaboration of overall morphology, territorial coverage, and morphological variance remains unclear (but see refs. 11 and 12).

By virtue of their essentially planar dendritic arborizations *in vivo* certain kinds of vertebrate neurons, such as retinal ganglion cells (RGCs) or cerebellar Purkinje cells, provide a simple system for studying the intrinsic nature of dendritic structure and the possible existence of growth strategies in a cell culture environment. For a variety of reasons, including those listed below, mammalian RGCs represent an attractive model system for addressing the role of intrinsic determinants of cellular morphology and physiology for these neurons: (*i*) In the intact retina, RGCs elaborate their dendritic arbors in what is essentially a two-dimensional space; therefore, a two-dimensional cell culture environment does not necessarily force a RGC to assume aberrant morphology (13, 14). (*ii*) Injection of tracers into the targets of RGC axons results in the retrograde labeling of RGC somata, thus allowing for the positive identification of the RGCs after dissociation of the retina (15). (*iii*) The exquisite lamination of the retina enables one to dissect away primarily the ganglion cell layer, thus providing primary cultures enriched in RGCs (16–18). (*iv*) The elaboration of individual RGC dendritic patterns is crucial for the functioning of the retina because the dendrites of these cells form biplanar dendritic sheets that subserve a variety of functions including the anatomical segregation of the well-described on and off channels in the retina (13, 14). (*v*) There is a well-described relationship between RGC dendritic structure and physiological function so that a study of the expression and intrinsic nature of RGC dendritic patterns has potential functional significance in the intact retina (19–23).

In the intact retina, the dendrites of RGCs aborize in essentially planar dendritic sheets that independently cover the retina. The formation of these dendritic sheets composed of individual RGC arbors depends on the ability of the *individual* arbors to fill in a restricted region of space (11). A powerful tool for assessing how well any geometrical structure fills in an available space is the Hausdorff dimension (H) of the structure (24, 25). This measure provides a metric for how well the RGC neurites fill in a bounded region of space and is scale independent. For the planar RGC neurite patterns elaborated in cell culture, the Hausdorff dimension is a number that varies continuously between 1 and 2. As the space-filling capacity of a neurite pattern increases, the Hausdorff dimension increases from a lower bound of 1 and approaches 2. To evaluate the intrinsic capacity for the expression of neuritic structure and the strategy used by postnatal RGCs for coverage of a spatially restricted region, we identified, isolated, and grew RGCs in cell culture. In addition, we applied this metric to the neurite arborizations of these cells during the reexpression of neuritic

The publication costs of this article were defrayed in part by page charge payment. This article must therefore be hereby marked "*advertisement*" in accordance with 18 U.S.C. §1734 solely to indicate this fact.

Abbreviation: RGC, retinal ganglion cell.
‡To whom reprint requests should be sent at the * address.

structure lacking interaction with other neurons and/or target tissue.

MATERIALS AND METHODS

RGCs in this study were obtained from kittens (postnatal age 1–8 weeks) used in ongoing electrophysiological experiments or from our closed breeding colony. Anesthesia was induced with a 35–40 mg/kg i.p. injection of sodium pentobarbitol (Nembutal). Multiple 1-μl injections of rhodamine-labeled latex microspheres (26) (Luma-Flor) were made into either the optic tract or the A layers of the dorsal lateral geniculate nucleus (15). The optic tract and the A layers of the dorsal lateral geniculate nucleus were located by electrophysiological recording before the injection of the microspheres. After a survival period of 48–72 hr, anesthesia was reinduced with vaporized methoxyfluothane (Fluothane) (0.6%–1.3%) in N_2O/O_2 (1:1). A femoral vein was cannulated, the eyeball was carefully removed, and a lethal dose of Nembutal (120 mg/kg) was administered into the femoral catheter. The retina was gently removed from the eyeball in a sterile calcium- and magnesium-free buffer solution and placed into an enzymatic solution (0.1% trypsin/0.5 mM EDTA in calcium- and magnesium-free Earle's balanced salt solution) to partially digest the connective tissue elements. After 12–17 min, the RGC layer was peeled from the retina as described (16–18). The layer was disrupted by gentle trituration followed by centrifugation at 40 × *g* for 5 min. Although the RGCs had achieved extensive dendritic branching before their removal from the retina (15, 27–30), centrifugation removed all processes from the RGCs before plating. The RGCs were resuspended in Hanks' balanced salt solution and plated onto glass coverslips coated with either poly(L-lysine), poly(D-lysine), or Cell-Tak (Biopolymers, Farmington, CT). Other substrates, such as uncoated glass, uncoated plastic, and fibronectin-coated glass, were tried, but the RGCs did not successfully attach and grow under these conditions. A mitotic inhibitor (cytosine arabinofuranoside at 10 μM) was added 12–24 hr after initial plating.

After cells attached to the coverslips, the coverslips were introduced into culture vessels containing a preestablished layer of rat astrocytes as a feeder layer (31, 32). The coverslips were equipped with pedestals isolating the retinal neurons from the rat astrocytes (32). The astrocytes were maintained in basal Eagle's medium with 10% fetal bovine serum until 1.5 days before introduction of the retinal neurons. At that time, the medium was changed to HB101 (DuPont) supplemented with 0.5–1% fetal bovine serum, 20 mM D-glucose, L-glutamine at 50 mg/100 ml, 26 mM bicarbonate, and 20–25 mM K^+. The elevated potassium levels and astrocytes were required to support the neuron growth for >3 days (33–36). The culture vessel was placed in an incubator that surrounded the stage of an inverted microscope. The environment was maintained at 36.0–36.5°C and 5% CO_2. The microscope was equipped with phase-contrast optics and a Dage MTI series 68 video camera that provided 1024 horizontal scan lines. Output of the camera was recorded with a Panasonic AG6010 time-lapse video cassette recorder that provided 300 horizontal scan lines. Video frames were collected at rates between 1 frame every 4 sec and 1 frame every 1.8 sec.

Two approaches were used to follow RGC growth: (*i*) Single labeled cells were followed longitudinally by continuous recording on the time-lapse video (six cells), or (*ii*) at a given time after plating, every coverslip from a particular dissociation was fixed (5% acetic acid/95% ethanol or 2% paraformaldehyde/0.5 M phosphate buffer), and cells on the coverslips were videotaped. This second method was preceded by systematically videotaping the labeled cells before fixation to observe short-term growth and record relative positions of the labeled cells before fixation. Video images were captured from the video tape with a frame grabber, and overlay drawings of the RGCs were made directly from the video images and stored in a computer. Lack of interaction with other retinal cells was possible because the cultures were extremely sparse (<4 cells per mm^2), and the pedestals kept RGCs completely isolated from the rat astrocyte monolayer.

All quantitative analysis, including the estimate of the Hausdorff dimension (H), was done automatically by using the stored overlay drawings (see Fig. 5 legend for details). In some analyses, multiple neurite patterns from a single actively growing RGC were used because the patterns showed significantly different structure as measured by the Hausdorff dimension, the total neurite length, and/or the number of interbranchpoint segments. This approach yielded a total of 75 neurite patterns for analysis. Video images of 18 camera lucida drawings of RGCs (*in vivo*) taken from published literature (23, 27, 30) were used to produce overlay drawings for these cells. These overlays were drawn in the same manner as the overlays produced for the cultured cells. This cell group from intact retinal preparations included one embryonic day-60 cell, four postnatal day-0 cells, three postnatal day-5 cells, three postnatal day-15 cells, and seven adult cells. The Hausdorff dimension was then calculated for this group of *in vivo* cells to compare with the cultured RGCs.

RESULTS

A freshly plated, fluorescently labeled RGC is illustrated in Fig. 1 *a* and *b*. Approximately 5–6 hr after the RGCs were initially plated, a subset (10–15%) of the labeled cells showed evidence of flattened lamellipodia about their perimeter (Fig. 1 *c* and *d* show a labeled RGC after 7 hr in culture). This stage was followed by coalescence of the lamellipodia into phase-dark processes that extended centrifugally in an intermittent fashion at ≈10–15 μm per day. Within 3–7 days, the cells developed characteristic branching patterns reminiscent of RGCs seen *in vivo* in postnatal cats (Figs. 1 *e* and *g*; 2 *a–d*). In control experiments where neurons from other sites (e.g., cerebral cortex and thalamus) were grown under identical conditions, the neurons formed neurite patterns radically different from those of the RGCs as assessed by a variety of criteria (Fig. 3 and see below). This example is typical of more than two-thirds of the cortical neurons from control experiments. Although cells with stellate morphology were also seen in the cortical cultures, no RGC was ever seen to express pyramidal structure. Additionally, the cortical neurons (especially those with stellate-like structure) did not survive well in the low-density and low-serum conditions of the RGC culture system.

The strategy by which the RGCs developed their neuritic patterns and established territory was evaluated by assessing how the RGCs increased and decreased the total neurite length of their arbors and the contribution of these changes to the space-filling capacity of the neurite patterns. In time-lapse analysis of individual RGCs (n = 6), the total neurite length paralleled the change in the number of interbranchpoint segments formed. The parallel trend between the total neurite length and the number of interbranchpoint segments was corroborated by quantifying the relationship between total neurite length and number of neuritic branches (Fig. 4*a*, r = 0.92, slope = 7.17) for a larger sample of RGCs (n = 48) independent of culture time (culture time varied from 0 to 18 days after plating). The mean interbranchpoint segment length for any given cell was stable after ≈3-day culture (x = 11.72 μm, SD = 2.9 μm, n = 67). This stability is reflected in the linear relationship illustrated in Fig. 4 *A*. The only instability in this unimodal linear relationship is exhibited by RGCs in culture for <2 days (see legend for Fig. 4*A*). These observations indicate that changes in the RGC total neurite length resulted predominantly from changes in the number of

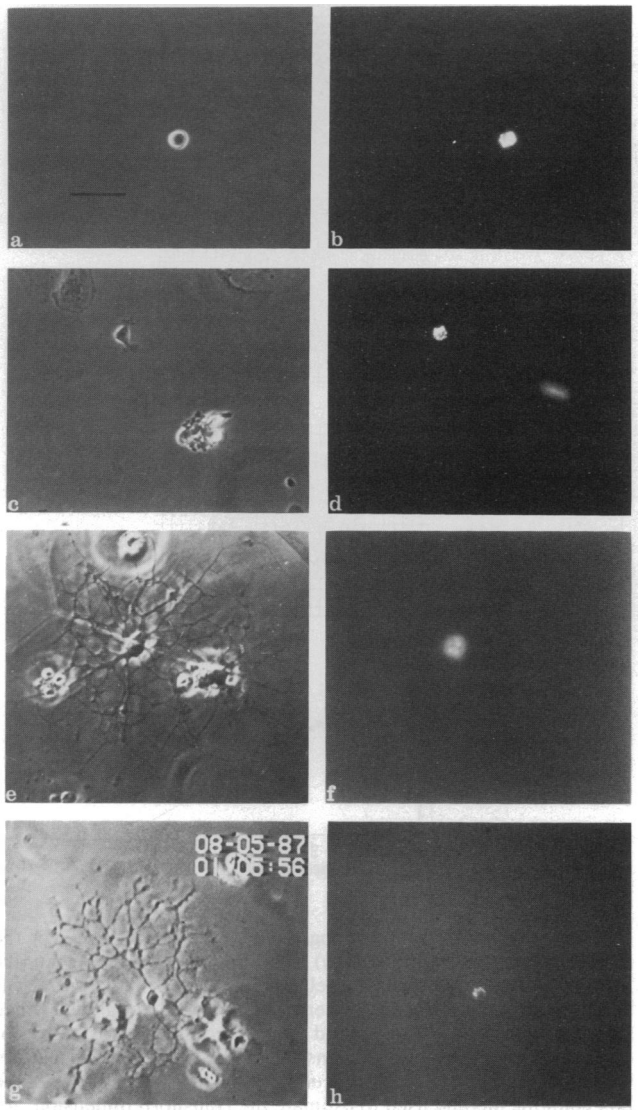

FIG. 1. Representative structure of retinal ganglion cells in culture. (*a*, *c*, *e*, and *g*) Phase-contrast photomicrographs of identified RGCs (taken from retinae of cats of postnatal age 2–8 weeks) that have redeveloped in cell culture; photomicrographs were taken at 2.5 hr, 7 hr, 8 days, and 10 days after plating, respectively. (*b*, *d*, *f*, and *h*) Fluorescence photomicrographs of the same cells. Cells in *a* and *c* on poly(L-lysine)-coated plastic culture dishes between circular islands of astrocytes, and cells in *e* and *g* are growing on Cell-Tak (Bioplymers)-coated 16-mm glass coverslips equipped with paraffin pedestals and resting on a confluent feeder layer of astrocytes derived from rat cerebral cortex (32). A small subset of cells ($n = 8$) included in this study was grown on poly(L-lysine)-coated Falcon primaria culture dishes between circular islands of rat astrocytes that were surrounded by Vaseline. Notice the unlabeled nonneuronal cells in *c*. *g* and *h* were taken directly off the video screen. (Bar = 40 μm.)

interbranchpoint segments of some stable mean length rather than from elongation and retraction of existing segments.

To test whether an intrinsic strategy existed for neurite coverage of a spatially restricted region, we assessed the contributions of total neurite length (T) and number of interbranchpoint segments (N) to the Hausdorff dimension (H) for all neurite patterns ($n = 75$) generated by the RGCs (Figs. 4*B* and 5). The relationship revealed an intrinsic strategy for covering a two-dimensional territory. Neurite patterns that efficiently fill space (as assessed by having higher H values—e.g., 1.60–1.88) can vary considerably in their total number of interbranchpoint segments or total

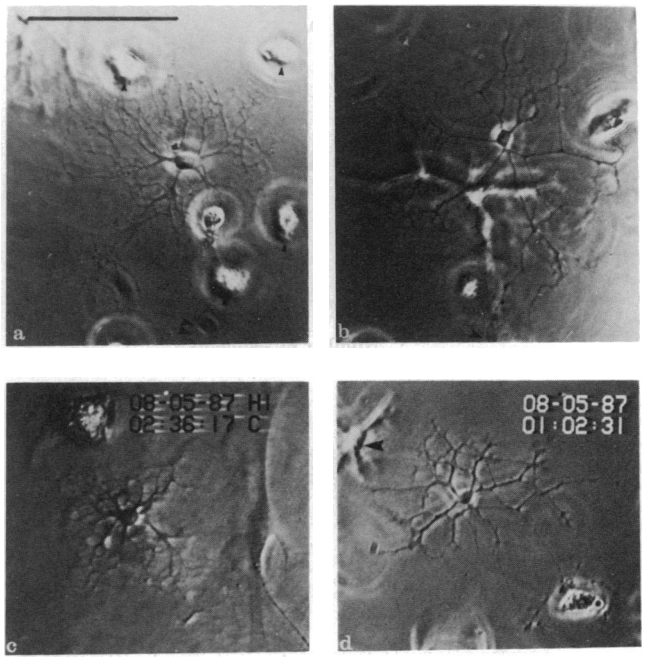

FIG. 2. Range of structure after significant branching has occurred. (*a*–*d*) Images of RGCs, all postively identified by retrograde labeling, growing on coverslips above the rat astrocyte layer; *a*, *c*, and *d* are 10-day cultures, whereas *b* is an 8-day culture. *b* and *d* were grown on coverslips coated with poly(L-lysine) ($M_r = 70{,}000$, Sigma), and *a* and *c* were grown on coverslips coated with 3 μg of Cell-Tak. *a* and *b* are photomicrographs, and *c* and *d* are photographs taken directly from a video monitor. Long axon-like processes were present on the cells in *a* (double arrowheads) and *b* (arrowhead at bottom). The smaller arrowheads in *a* and *b* point to cells growing on the opposite side of the coverslip; likewise, the arrowhead in *d* indicates a cell growing on the opposite side of the coverslip. RGCs did not grow on uncoated glass coverslips, and there was no significant effect of substrate [Cell-Tak vs. poly(L-lysine)] on the Hausdorff dimension of the neurite patterns (two-tailed Mann–Whitney U test: $U = 318$, $n_1 = 24$, $n_2 = 44$; $P = 0.007$).

neurite length. Thus, the RGC neurites do not fill space simply by adding new segments of some stable mean length or by simply increasing the total neurite length of the neurite pattern. Instead, they achieve a relatively uniform coverage of a restricted territory by the strategic selection of length, location, and orientation of individual interbranchpoint seg-

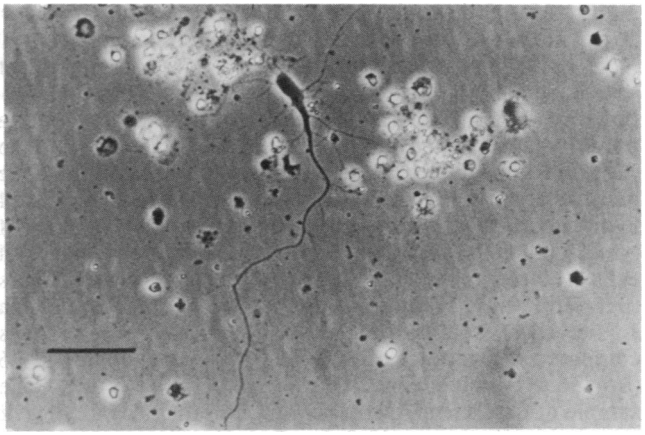

FIG. 3. Rat cortical neuron grown under identical conditions as the RGCs. Rat cortical neuron after 3-day culture growing on a coverslip over an astrocyte feeder layer. Conditions were identical to those used for RGCs. Rat cortical neurons were derived from embryonic rats between embryonic day 16 and 18. (Bar = 50 μm.)

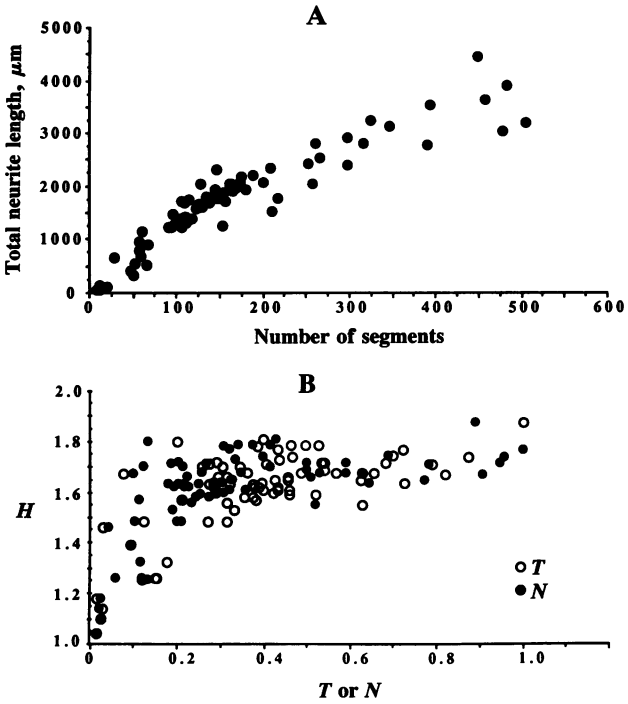

FIG. 4. (*A*) Scatter plot of the total neurite length of the neuritic arbors versus the number of segments belonging to each arbor independent of time in culture. Although total neurite length decreases rapidly as number of segments drops below ≈55–65, a linear trend between these two parameters is exhibited ($r = 0.92$, slope = 7.17). The nonlinearity can be partially accounted for by observing that most (7/12) cells that possess <60 segments belong to the 0- to 48-hr group—a time when the neurites are not as consistently successful in extending processes as later. During this period one or a few segments commonly extend much farther than average and, hence, represent a greater proportion of total segment length. Nonlinearity in this range can be attributed to the establishment or loss of one or more of these longer-than-average segments. With increasing culture time, this effect was not as dominant. (*B*) Plot of the Hausdorff dimension H versus the normalized total neurite length T and the normalized number of segments N for every neurite pattern analyzed. All three of these variables were normalized to the largest value obtained in the population of 75 neurite patterns. Number of segments ranged from 8 to 506; total neurite length ranged from 56 to 3234 μm. The Hausdorff dimensions ranged from 1.04 to 1.88. After 3-day culture, the Hausdorff dimension ranged from 1.32 to 1.88 ($\bar{x} = 1.66$, SD = 0.10, $n = 56$).

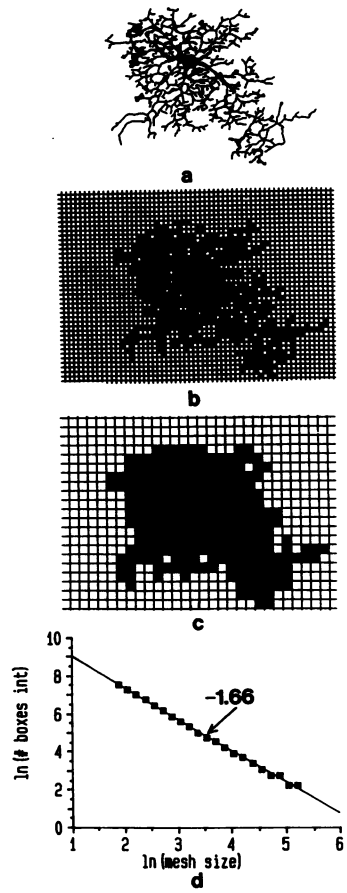

FIG. 5. Method of calculating the Hausdorff dimension of the neurite patterns of the RGCs. (*a*) Line drawing of a representative RGC after 10-day culture (same cell as Fig. 2*c*). This line drawing was made directly from a stored overlay drawing of a digitized video image of the RGC. The stored overlay drawing was used for calculating the Hausdorff dimension of the RGC neurite pattern (somata were not used in this calculation). (*b* and *c*) Illustration of the box counting method used to estimate the Hausdorff dimension. An interactive computer program covered the stored overlay drawing with a sequence ($n > 20$) of grids composed of square boxes of side equal to m. For each grid (characterized by the box or mesh size), the number of boxes intersected by the overlay drawing was counted and stored in the computer. To avoid biasing box count due to grid (square mesh) geometry, position and orientation of the overlay drawing were randomly varied relative to the grid. At each particular mesh size, this procedure was done 10 times, and the number of boxes intersected was averaged. Thus, a relationship between mesh size and average number of boxes intersected was established. The logarithm of the number of boxes intersected [ln (# boxes int)] was plotted against the logarithm of mesh size; negative of the slope of the regression line for this plot yields the Hausdorff dimension of the neurite pattern (1.66 in this example). In *b* and *c*, the intersected boxes were filled to illustrate the method. This method for estimating Hausdorff dimension follows from the definition of Hausdorff dimension (24, 25). (*d*) Plot of logarithm of number of boxes intersected versus logarithm of mesh size for the cell in *a*. Because we had no *a priori* knowledge that the processes producing the neurite patterns would generate structures that yield logarithmic normally distributed variations in the average box count as a function of mesh size, we did not include confidence-interval estimates for the regression-line slope.

ments. After 3-day culture, most neurite patterns (77%, n = 56 neurite patterns) achieve relatively uniform coverage ($1.60 < H < 1.88$) of a territory independent of the amount of "working material" (total neurite length or number of interbranchpoint segments) available. During this same period, a minority (23%) of neurite patterns have H values from 1.32 to 1.59 and appear sparser in their territorial coverage. The neurites of any individual RGC exhibited a high degree of self avoidance with self intersections occurring at a frequency of ≈0.5% (20 cells, n = 2500 interbranchpoint segments). All cells in culture for >3 days had neuritic arbors with diameters between 110 and 270 μm. For the *in vivo* cells, H ranged from 1.54 to 1.94 with an average of 1.73 (n = 18, SD = 0.12) as compared with a range of 1.32 to 1.88 and an average of 1.66 (n = 56, SD = 0.10) for RGCs in culture for >3 days. The sample of RGCs from intact preparations included a range of morphological classes (10 β, 6 α, 2 γ). For direct comparison of the morphology and coverage of a RGC grown in culture to one studied *in vivo*, note the similarity between the cell in Fig. 5 to the P3 cell in Figure 8*A* in Ramoa *et al.* (15). The H values for these RGCs were 1.66 and 1.59, respectively. In control experiments, neurons derived from other regions of the central nervous system (see above) followed a different pattern of growth. These neurons exhibited frequent self-crossings, and their growth strategy was dominated by neurite extension. In addition, these neurons filled space much less efficiently than RGCs with H values consistently <1.3 independent of the time in culture.

DISCUSSION

These experiments show that postmitotic (37, 38) mammalian neurons that have already achieved extensive dendritic differentiation *in vivo* (15, 27–30) can reexpress emergent structural features *in vitro* characteristic and reminiscent of the *in vivo* condition. This reexpression is independent of factors from other cells normally present in the immediate locale of the RGCs in the intact retina and is independent of interactions with target tissue. The most striking feature of the expression of the neuritic structure of these cells is the existence of an apparent growth strategy that operated more or less independently of number (or amount) of neurites expressed. Modulation of the number of neurite segments having a stable mean length and the strategic selection of their position, orientation, and length produced relatively uniform territorial coverage, as assessed by the Hausdorff dimension, and yet generated rich morphological variance (Figs. 1 *e* and *g*; 2 *a–d*).

Existence of this morphological variance is obvious upon casual inspection of the cells and is implicit in the observation that the space-filling capacity was independent of the number of interbranchpoint segments and the total neurite length (Fig. 2). Hence, once a RGC has survived for >3 days in culture and established neuritic branches, its space-filling capacity (H) will probably (77%) fall between 1.6 and 1.9 and be independent of the amount of "working material" available. The fraction of RGCs with low H values (<1.6) declines with time in culture from 50% at <72 hr to 23% for cells in culture for >72 hr. The first 72 hr in culture is an exceptional period in that rapid changes in the space-filling capacity (H) of the neurites occur because the RGCs are not as consistently successful at extending and maintaining neurites as they are at later times (see legend for Fig. 4*A*). The observation that uniform territorial coverage is more or less independent of the amount of "working material" is consistent with the high degree of self avoidance of the neurites and the limited diameters of the neurite patterns. However, the mere existence of these two phenomena do not establish a causal relationship with the strategy of uniform coverage. A variety of growth schemes employing only self-avoidance and/or a limited period of growth could allow for the emergence of uniform coverage of a 2-dimensional territory.

This study provides evidence for the intrinsic capabilities of individual RGCs to elaborate an emergent cellular trait. However, extrinsic factors clearly play a role in the development and maintenance of the dendritic arbors of RGCs in the mammalian retina. The structure of RGC dendritic arbors from cat and rat has been shown *in vivo* to exhibit a sensitivity and plasticity to the proximity and branching patterns of neighboring ganglion cells after perturbations that significantly disrupt these neighbor-dependent relationships (11, 12, 39, 40). It has recently been suggested that transient morphological features of developing RGCs subserve some form of dendritic competition (12, 15, 28). In view of the demonstrated sensitivity to external perturbations, it is noteworthy that the cultured RGCs expressed a range of structure in such a homogeneous environment. This intrinsic structural variance constrained by a common mode of covering territory may allow for the emergence of the diverse morphological and functional classes of RGCs in the retina that are later shaped by epigenetic influences, such as the presence and activity of afferent input. How the intrinsic capacity and strategy for elaborating neuritic structure depends on developmental age and epigenetic influences from neighboring RGCs and target tissue is an interesting question awaiting a more precise answer.

We thank the University of Alabama at Birmingham Neurobiology Research Center Cell Reconstruction Facility, Drs. Lee Ann Coleman and Yves Fregnac for comments and suggestions on the manuscript, Kevin Ramer for software development, and Wanda Smith for word processing. This work was supported by National Science Foundation Grant BNS 8720069.

1. Ramon y Cajal, S., *Degeneration and Regeneration of the Nervous System* [May, R. M., trans. (1928) (Oxford Univ. Press, London)].
2. Cowan, W. M. (1978) *Int. Rev. Physiol.* **17**, 150–191.
3. Scott, B. E., Engelbert, V. E. & Fisher, K. C. (1969) *Exp. Neurol.* **23**, 230–248.
4. Fishbach, G. (1970) *Science* **169**, 1331–1333.
5. Banker, G. A. & Cowan, W. M. (1977) *Brain Res.* **126**, 397–425,
6. Dichter, M. A. (1978) *Brain Res.* **149**, 279–293.
7. Banker, G. A. & Cowan, W. M. (1979) *J. Comp. Neurol.* **187**, 469–494.
8. Kriegstein, A. R. & Dichter, M. A. (1983) *J. Neurosci.* **3**, 1634–1647.
9. Banker, G. A. & Waxman, A. B. (1988) in *Intrinsic Determinants of Neuronal Form and Function*, eds. Lasek, R. J. & Black, M. M. (Liss, New York), pp. 61–82.
10. Lasek, R. J. (1988) in *Intrinsic Determinants of Neuronal Form and Function*, eds. Lasek, R. J. & Black, M. M. (Liss, New York), pp. 1–58.
11. Wassle, H., Peichl, L. & Boycott, B. B. (1981) *Nature (London)* **292**, 344–345.
12. Perry, V. H. & Linden, R. (1982) *Nature (London)* **297**, 683–685.
13. Dowling, J. (1987) *The Retina* (Belknap–Harvard Univ. Press, Cambridge, MA).
14. Famiglietti, E. V. & Kolb, H. (1976) *Science* **194**, 193–195.
15. Ramoa, A. S., Campbell, G. A. & Shatz, C. J. (1988) *J. Neurosci.* **8**, 4239–4261.
16. Shiosaka, S., Kiyama, K. & Tohyama, M. (1984) *J. Neurosci. Methods* **10**, 229–235.
17. Montague, P. R. & Friedlander, M. J. (1987) *Soc. Neurosci. Abstr.* **13**, 1299.
18. Montague, P. R. & Friedlander, M. J. (1988) *Soc. Neurosci. Abstr.* **14**, 459.
19. Saito, H.-A. (1983) *J. Comp. Neurol.* **221**, 279–288.
20. Amthor, F. (1984) *Brain Res.* **298**, 187–190.
21. Fukuda, Y., Hasaio, C. F. & Watanabe, M. (1984) *J. Neurophysiol.* **52**, 999–1013.
22. Stanford, L. R. & Sherman, S. M. (1984) *Brain Res.* **297**, 381–386.
23. Stanford, L. R. (1987) *J. Neurophysiol.* **58**, 940–964.
24. Mandelbrot, B. B. (1982) *The Fractal Geometry of Nature* (Freeman, San Francisco).
25. Falconer, K. J. (1986) *Geometry of Fractal Sets* (Cambridge Univ. Press, Cambridge, MA).
26. Katz, L. C., Burkhalter, A. & Dreyer, W. J. (1984) *Nature (London)* **310**, 498–500.
27. Maslim, J., Webster, M. & Stone, J. (1986) *J. Comp. Neurol.* **254**, 382–402.
28. Ramoa, A. S., Campbell, G. A. & Shatz, C. J. (1987) *Science* **237**, 522–525.
29. Dann, J. F., Buhl, E. H. & Peichl, L. (1987) *Neurosci. Lett.* **80**, 21–26.
30. Dann, J. F., Buhl, E. H. & Peichl, L. (1988) *J. Neurosci.* **8**, 1485–1499.
31. McCarthy, K. D. & deVellis, J. (1980) *J. Cell Biol.* **85**, 890–902.
32. Banker, G. A. (1980) *Science* **209**, 809–810.
33. Scott, B. S. & Fisher, K. C. (1970) *Exp. Neurol.* **27**, 16–22.
34. Scott, B. S. & Fisher, K. C. (1971) *Exp. Neurol.* **31**, 183–188.
35. Scott, B. S. (1976) *J. Cell. Physiol.* **91**, 305–316.
36. Bennett, M. R. & White, W. (1979) *Brain Res.* **173**, 549–553.
37. Johns, P. R., Rusoff, A. C. & Dubin, M. W. (1979) *J. Comp. Neurol.* **187**, 545–556.
38. Walsh, C., Polley, E. H., Hickey, T. L. & Guillery, R. W. (1983) *Nature (London)* **302**, 611–613.
39. Eysel, U. L., Peichl, L. & Wassle, H. (1985) *J. Comp. Neurol.* **242**, 134–145.
40. Leventhal, A. G., Schall, J. D. & Ault, S. J. (1988) *J. Neurosci.* **8**, 2028–2038.